

SUSY-QCD Effect on Top-Charm Associated Production at Linear Collider

Chong Sheng Li ^a, Xinmin Zhang ^b and Shou Hua Zhu ^{c,d}

^a Department of Physics, Peking University, Beijing 100871, P.R. China

^b Institute of High Energy Physics, P.O. Box 918(4), Beijing 100039, P.R. China

^c CCAST (World Lab), P.O. Box 8730, Beijing 100080, P.R. China

^d Institute of Theoretical Physics, Academia Sinica, P.O. Box 2735, Beijing 100080, P.R. China

ABSTRACT

We evaluate the contribution of SUSY-QCD to top-charm associated production at next generation linear colliders. Our results show that the production cross section of the process $e^+e^- \rightarrow t\bar{c}$ or $\bar{t}c$ could be as large as 0.1 fb, which is larger than the prediction of the SM by a factor of 10^8 .

One of the most important physics in top quark sector is to probe anomalous flavor changing neutral current (FCNC) couplings. In the Standard Model (SM), FCNC couplings are forbidden at the tree level and much suppressed in loops by the GIM mechanism. Any signals on FCNC couplings in the processes of top quark decay and productions or indirectly in loops will indicate the existence of new physics beyond the SM. Recently in the framework of effective lagrangian, Han and Hewett [1] have examined carefully the possibility of exploring the FCNC couplings $tcZ/tc\gamma$ in the production vertex for the reaction $e^+e^- \rightarrow t\bar{c} + \bar{t}c$ and concluded that at higher energy colliders with $0.5 - 1$ TeV center-of-mass energy, the resulting sensitivity to FCNC couplings will be better than the present constraints [2]. In this paper, in the minimal supersymmetric standard model (MSSM) we study the process $e^+e^- \rightarrow t\bar{c} + \bar{t}c$ and perform an detail calculation of the contribution from the FCNC couplings in the vertex of gluino-squark-quark to the production cross section. We will point out that at higher energy e^+e^- colliders the cross section could be as large as 0.1 fb which is at least eight order of magnitude larger than the prediction of the SM $\sim 10^{-10} - 10^{-9}$ fb [3].

The MSSM is arguably the most promising candidate for physics beyond the SM. Beside many attractive features of supersymmetry in understanding the mass hierarchy, gauge coupling unification, the weak scale SUSY models in generally lead to a rich flavor physics. In fact, SUSY models often have arbitrary flavor mixings and mass parameters in the squark and slepton sectors and these mass matrices after diagonalization induce FCNC couplings at tree level in the vertex of gluino-squark-quark *etc.* Phenomenologically one would have to assume certain symmetries or dynamical mechanisms to prevent large FCNC among the first and second generations. On the other hand the flavor structure, especially among the second and third generations in the SUSY sector motivates us to seek for new physics and any experimental observation on the FCNC processes beyond the SM would undoubtedly shed light on our understanding for flavor physics. In this paper we take model of Ref. [4,5] where the FCNC couplings relevant to our calculation is given by:

$$\mathcal{L}_{\mathcal{FC}} = -\sqrt{2}g_s T^a K \bar{g} P_L q \tilde{q}_L + h.c. \quad (1)$$

In (1), K is the supersymmetric version of the Kobayashi–Maskawa matrix, which is explicitly expressed as:

$$K_{ij} = \begin{pmatrix} 1 & \varepsilon & \varepsilon^2 \\ -\varepsilon & 1 & \varepsilon \\ -\varepsilon^2 & -\varepsilon & 1 \end{pmatrix} \quad (2)$$

where ε parameterizes the strength of flavor mixing and is shown to be as large as $1/2$ without contradicting with the low energy experimental data [5].

In Fig.(1) we give the Feynman diagrams for the process $e^+(p_1)e^-(p_2) \rightarrow t(k_1)\bar{c}(k_2)$. In calculations, we have neglected the scalar u-quark contribution since it is highly suppressed by $K_{12}K_{13}$; and we use the dimensional regularization to control the ultraviolet divergence. We have checked that all divergences cancel out in the final result with the summing up of all of the diagrams. The calculations are carried out in the frame of the center of mass system (CMS) and Mandelstam variables have been employed:

$$s = (p_1 + p_2)^2 = (k_1 + k_2)^2 \quad t = (p_1 - k_1)^2 \quad u = (p_1 - k_2)^2. \quad (3)$$

After a straightforward calculations, one obtains for the amplitudes

$$M = \frac{e}{S} \bar{v}(p_1) \gamma_\mu u(p_2) \bar{u}(k_1) V^\mu(tc\gamma) v(k_2) + \frac{g}{2 \cos \theta_W (S - M_Z^2)} \bar{v}(p_1) \gamma_\mu (g_V^e - g_A^e \gamma_5) u(p_2) \bar{u}(k_1) V^\mu(tcZ) v(k_2) \quad (4)$$

where, $g_V^e = 1/2 - 2 \sin^2 \theta_W$, $g_A^e = 1/2$, and $V^\mu(tc\gamma)$ and $V^\mu(tcZ)$ are the on-shell quarks effective vertices given by *

$$V^\mu(tc\gamma; Z) = f_1^{\gamma;Z} \gamma_\mu P_R + f_2^{\gamma;Z} \gamma_\mu P_L + f_3^{\gamma;Z} k_{1\mu} P_R + f_4^{\gamma;Z} k_{1\mu} P_L + f_5^{\gamma;Z} k_{2\mu} P_R + f_6^{\gamma;Z} k_{2\mu} P_L. \quad (5)$$

The form factors, $f_i^{\gamma;Z}$ are

$$f_1^\gamma = \sum_{\tilde{q}=\tilde{c},\tilde{t}} \frac{(\pm 1) \epsilon e g_s^2 \cos(\theta_{\tilde{q}}) \sin(\theta_{\tilde{q}}) m_{\tilde{g}}}{12 m_t \pi^2} [B_0(0, m_{\tilde{g}}^2, m_{\tilde{q}_2}^2) - B_0(m_t^2, m_{\tilde{g}}^2, m_{\tilde{q}_2}^2)] + R.R.$$

$$f_2^\gamma = \sum_{\tilde{q}=\tilde{c},\tilde{t}} \frac{(\pm 1) \epsilon e g_s^2 \sin^2(\theta_{\tilde{q}})}{24 m_t^2 \pi^2} [(m_{\tilde{g}}^2 - m_{\tilde{q}_2}^2) B_0(0, m_{\tilde{g}}^2, m_{\tilde{q}_2}^2) - (m_{\tilde{g}}^2 - m_{\tilde{q}_2}^2 + m_t^2) B_0(m_t^2, m_{\tilde{g}}^2, m_{\tilde{q}_2}^2)]$$

*For simplicity, we only give the results in the limit of $m_c = 0$. However in our numerical calculations, we use the full formulas.

$$\begin{aligned}
& +4m_t^2 C_{00}] + R.R. \\
f_3^\gamma &= \sum_{\tilde{q}=\tilde{c},\tilde{t}} \frac{(\mp 1)\epsilon e g_s^2 \sin(\theta_{\tilde{q}}) \cos(\theta_{\tilde{q}}) m_{\tilde{g}}}{12\pi^2} [C_0 + 2C_1] + R.R. \\
f_4^\gamma &= \sum_{\tilde{q}=\tilde{c},\tilde{t}} \frac{(\pm 1)\epsilon e g_s^2 \sin(\theta_{\tilde{q}}) \cos(\theta_{\tilde{q}}) m_{\tilde{g}}}{12\pi^2} [C_0 + 2C_2] + R.R. \\
f_5^\gamma &= \sum_{\tilde{q}=\tilde{c},\tilde{t}} \frac{(\pm 1)\epsilon e g_s^2 \sin^2(\theta_{\tilde{q}}) m_t}{12\pi^2} [C_0 + 2C_{11}] + R.R. \\
f_6^\gamma &= \sum_{\tilde{q}=\tilde{c},\tilde{t}} \frac{(\mp 1)\epsilon e g_s^2 \sin^2(\theta_{\tilde{q}}) m_t}{12\pi^2} [C_0 + 2C_{12}] + R.R. \tag{6}
\end{aligned}$$

$$\begin{aligned}
f_1^Z &= \sum_{\tilde{q}=\tilde{c},\tilde{t}} \frac{(\mp 1)\epsilon g g_s^2 \sin^2(\theta_w) \cos(\theta_{\tilde{q}}) \sin(\theta_{\tilde{q}})}{12m_t \cos(\theta_w) \pi^2} [B_0(0, m_{\tilde{g}}^2, m_{\tilde{q}_2}^2) - B_0(m_t^2, m_{\tilde{g}}^2, m_{\tilde{q}_2}^2)] + R.R. \\
f_2^Z &= \sum_{\tilde{q}=\tilde{c},\tilde{t}} \frac{(\mp 1)\epsilon g g_s^2 \sin^2(\theta_{\tilde{q}})}{96m_t^2 \cos(\theta_w) \pi^2} \{(-3 + 4 \sin^2(\theta_w))[(m_{\tilde{g}}^2 - m_{\tilde{q}_2}^2)B_0(0, m_{\tilde{g}}^2, m_{\tilde{q}_2}^2) \\
& - (m_{\tilde{g}}^2 - m_{\tilde{q}_2}^2 + m_t^2)B_0(m_t^2, m_{\tilde{g}}^2, m_{\tilde{q}_2}^2)] + 4m_t^2(-3 \sin^2(\theta_{\tilde{q}}) + 4 \sin^2(\theta_w))C_{00} \\
& - 12m_t^2 \cos^2(\theta_{\tilde{q}})\hat{C}_{00}\} + R.R. \\
f_3^Z &= \sum_{\tilde{q}=\tilde{c},\tilde{t}} \frac{(\pm 1)\epsilon g g_s^2 \sin(\theta_{\tilde{q}}) \cos(\theta_{\tilde{q}}) m_{\tilde{g}}}{48 \cos(\theta_w) \pi^2} [(4 \sin^2(\theta_w) - 3 \sin^2(\theta_{\tilde{q}}))(C_0 + 2C_1) \\
& + 3 \sin^2(\theta_{\tilde{q}})(\hat{C}_0 + 2\hat{C}_1)] + R.R. \\
f_4^Z &= \sum_{\tilde{q}=\tilde{c},\tilde{t}} \frac{(\mp 1)\epsilon g g_s^2 \sin(\theta_{\tilde{q}}) \cos(\theta_{\tilde{q}}) m_{\tilde{g}}}{48 \cos(\theta_w) \pi^2} [(4 \sin^2(\theta_w) - 3 \sin^2(\theta_{\tilde{q}}))(C_0 + 2C_2) \\
& + 3 \sin^2(\theta_{\tilde{q}})(\hat{C}_0 + 2\hat{C}_2)] + R.R. \\
f_5^Z &= \sum_{\tilde{q}=\tilde{c},\tilde{t}} \frac{(\mp 1)\epsilon g g_s^2 \sin^2(\theta_{\tilde{q}}) m_t}{48 \cos(\theta_w) \pi^2} [(4 \sin^2(\theta_w) - 3 \sin^2(\theta_{\tilde{q}}))(C_0 + 2C_{11}) \\
& - 3 \cos^2(\theta_{\tilde{q}})(\hat{C}_0 + 2\hat{C}_{11})] + R.R. \\
f_6^Z &= \sum_{\tilde{q}=\tilde{c},\tilde{t}} \frac{(\pm 1)\epsilon g g_s^2 \sin^2(\theta_{\tilde{q}}) m_t}{48 \cos(\theta_w) \pi^2} [(4 \sin^2(\theta_w) - 3 \sin^2(\theta_{\tilde{q}}))(C_0 + 2C_{12}) \\
& - 3 \cos^2(\theta_{\tilde{q}})(\hat{C}_0 + 2\hat{C}_{12})] + R.R. \tag{7}
\end{aligned}$$

where $R.R.$ represents the replacement of $\theta_{\tilde{q}} \rightarrow \pi/2 + \theta_{\tilde{q}}$ and $m_{\tilde{q}_1} \leftrightarrow m_{\tilde{q}_2}$. The variables of three point functions C_i , C_{ij} [6] and \hat{C}_i , \hat{C}_{ij} are $(m_t^2, S, 0, m_{\tilde{g}}^2, m_{\tilde{q}_2}^2, m_{\tilde{q}_2}^2)$ and $(m_t^2, S, 0, m_{\tilde{g}}^2, m_{\tilde{q}_2}^2, m_{\tilde{q}_1}^2)$, respectively.

In the MSSM the mass eigenstates of the squarks \tilde{q}_1 and \tilde{q}_2 are related to the weak eigenstates \tilde{q}_L and \tilde{q}_R by [7]

$$\begin{pmatrix} \tilde{q}_1 \\ \tilde{q}_2 \end{pmatrix} = R^{\tilde{q}} \begin{pmatrix} \tilde{q}_L \\ \tilde{q}_R \end{pmatrix} \quad \text{with} \quad R^{\tilde{q}} = \begin{pmatrix} \cos \theta_{\tilde{q}} & \sin \theta_{\tilde{q}} \\ -\sin \theta_{\tilde{q}} & \cos \theta_{\tilde{q}} \end{pmatrix}. \quad (8)$$

For the squarks, the mixing angle $\theta_{\tilde{q}}$ and the masses $m_{\tilde{q}_{1,2}}$ can be calculated by diagonalizing the following mass matrices

$$\begin{aligned} M_{\tilde{q}}^2 &= \begin{pmatrix} M_{LL}^2 & m_q M_{LR} \\ m_q M_{RL} & M_{RR}^2 \end{pmatrix}, \\ M_{LL}^2 &= m_{\tilde{Q}}^2 + m_q^2 + m_z^2 \cos 2\beta (I_q^{3L} - e_q \sin^2 \theta_w), \\ M_{RR}^2 &= m_{\tilde{U}, \tilde{D}}^2 + m_q^2 + m_z^2 \cos 2\beta e_q \sin^2 \theta_w, \\ M_{LR} &= M_{RL} = \begin{cases} A_t - \mu \cot \beta & (\tilde{q} = \tilde{t}) \\ A_b - \mu \tan \beta & (\tilde{q} = \tilde{b}), \end{cases} \end{aligned} \quad (9)$$

where $m_{\tilde{Q}}^2, m_{\tilde{U}, \tilde{D}}^2$ are soft SUSY breaking mass terms of the left- and right-handed squark, respectively; μ is the coefficient of the $H_1 H_2$ term in the superpotential; A_t and A_b are the coefficient of the dimension-three tri-linear soft SUSY-breaking terms; I_q^{3L}, e_q are the weak isospin and electric charge of the squark \tilde{q} . From Eqs. 8 and 9, we have

$$\begin{aligned} m_{\tilde{t}_{1,2}}^2 &= \frac{1}{2} \left[M_{LL}^2 + M_{RR}^2 \mp \sqrt{(M_{LL}^2 - M_{RR}^2)^2 + 4m_t^2 M_{LR}^2} \right] \\ \tan \theta_{\tilde{t}} &= \frac{m_{\tilde{t}_1}^2 - M_{LL}^2}{m_t M_{LR}}. \end{aligned} \quad (10)$$

Now we present the numerical results. For the SM parameters, we take

$$\begin{aligned} m_Z &= 91.187 \text{ GeV}, \quad m_W = 80.33 \text{ GeV}, \quad m_t = 176.0 \text{ GeV}, \quad m_c = 1.4 \text{ GeV} \\ \alpha &= 1/128, \quad \alpha_S = 0.118 \end{aligned} \quad (11)$$

For the MSSM parameters, we choose $\mu = -100 \text{ GeV}$ and $\epsilon^2 = 1/4$. To simplify the calculation we have taken that $m_{\tilde{U}} = m_{\tilde{D}} = m_{\tilde{Q}} = A_t = m_S$ (global SUSY). In Figs. 2-5, we show the cross sections of the process $e^+ e^- \rightarrow t \bar{c}$ as functions of $m_S, m_{\tilde{g}}, \sqrt{s}$ and $\tan \beta$. One can see that the production cross section increases as squarks and gluino masses decrease, and it could reach 0.1 fb for favorable parameters. This is an enhancement by a factor of 10^8 relative to the SM prediction. Such enhancement could be easily understood as following:

$$\frac{\sigma_{SUSY}}{\sigma_{SM}} \sim \left(\frac{\alpha_s \Delta m_{\tilde{q}}^2}{\alpha m_b^2} \right)^2, \quad (12)$$

where $\Delta m_{\tilde{q}}^2$ represents the possible mass square difference among squarks. If $\Delta m_{\tilde{q}}^2$ varies from $100^2 - 200^2 (GeV)^2$, $\frac{\sigma_{SUSY}}{\sigma_{SM}} = 10^7 \sim 10^8$. At the same time, this kind of enhancement could also be observed in FCNC decay process of top quark [8]. Due to the rather clean experimental environment and well-constrained kinematics, the signal of $\bar{t}c$ or $t\bar{c}$ would be spectacular [1]. We expect the SUSY-QCD effects studied in this paper be observed at higher energy e^+e^- colliders.

ACKNOWLEDGMENTS

We thank Profs. Tao Han and Chao-Shang Huang for discussions. This work was supported in part by the National Natural Science Foundation of China, Doctoral Program Foundation of Higher Education, the post doctoral foundation of China, and a grant from the State Commission of Science and Technology of China. S.H. Zhu also gratefully acknowledges the support of K.C. Wong Education Foundation, Hong Kong.

-
- [1] T. Han and J. Hewett, hep-ph/9811237.
 - [2] R.D. Peccei, S. Peris and X. Zhang, Nucl. Phys. B349, 305 (1991); T. Han, R.D. Peccei and X. Zhang, Nucl. Phys. B454, 527 (1995); T. Han et al, Phys. Rev. D55, 7241 (1997).
 - [3] C.S. Huang, X.H. Wu and S.H. Zhu, Phys. Lett. B452 (1999) 143 and references there-in.
 - [4] J. Ellis and D.V. Nanopoulos, Phys.Lett **110B**(1982)44; R. Barbieri and R. Gatto, Phys.Lett**110B** (1982)211; T. Inami and C.S. Lim, Nucl.Phys.**B207** (1982)533; B.A. Campbell, Phys. Rev.**D28**(1983)209; M.J. Duncan, Nucl.Phys.**B221**(1983)221; J.F. Donoghue, H.P. Nilles and D. Wyler, Phys.Lett.**128 B**(1983)55.
 - [5] M.J. Duncan, Phys.Rev.**D31**(1985)1139.

- [6] G. Passarino and M. Veltman, Nucl. Phys. B 33, 151 (1979); R. Mertig, M. Bohm and A. Denner, Comp. Phys. Comm. 64, 345 (1991); A. Denner, Fortschr. Phys. 41, 307 (1993).
- [7] H.E. Haber and G.L. Kane, Phys.Rep. **117**, 75(1985); J.F. Gunion and H.E. Haber, Nucl. Phys. **B272**, 1(1986) For a review see, e.g. J.F. Gunion et.al., Higgs Hunter's Guide (Addison-Wesley, MA,1990).
- [8] To see for examples, C.S. Li, R.J. Oakes and J.M. Yang, Phys. Rev. **D49**, 293 (1994), Erratum-*ibid.* **D56**, 3156 (1997); J.M. Yang, B.-L. Young and X. Zhang, Phys. Rev. **D58**, 055001 (1998); J.-M. Yang and C.-S. Li, Phys. Rev. **D49**, 3412 (1994), Erratum-*ibid.* **D51**, 3974 (1995); G. Eilam, J.L. Hewett and A. Soni, Phys. Rev. **D44**, 1473 (1991); Erratum-*ibid.* **D59**:039901,1999.

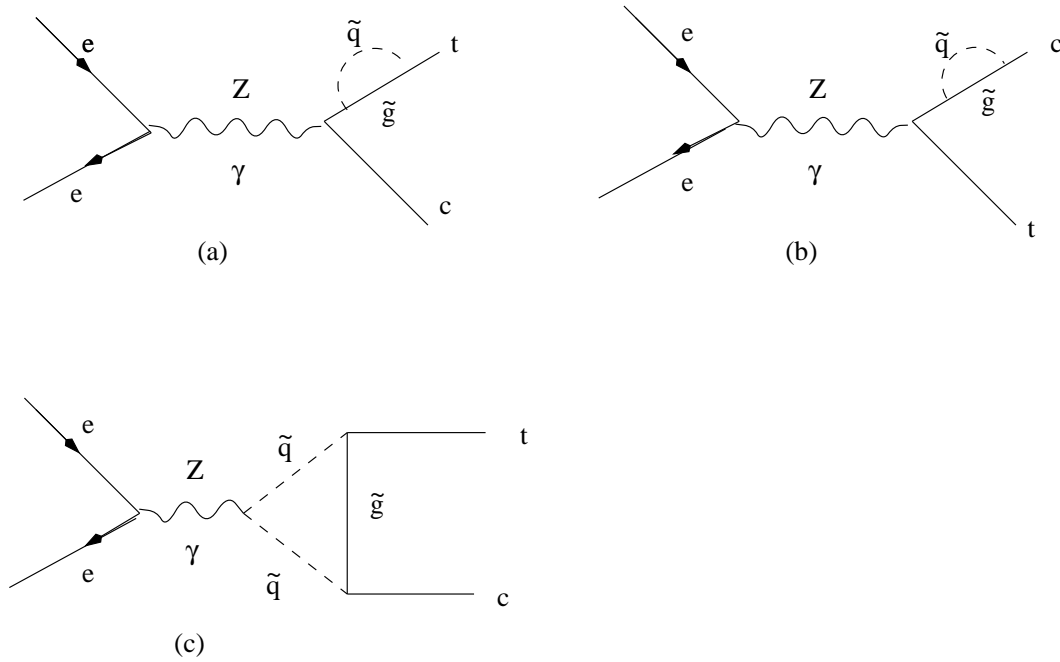


FIG. 1. The Feynmann diagrams for the process $e^+e^- \rightarrow t\bar{c}$.

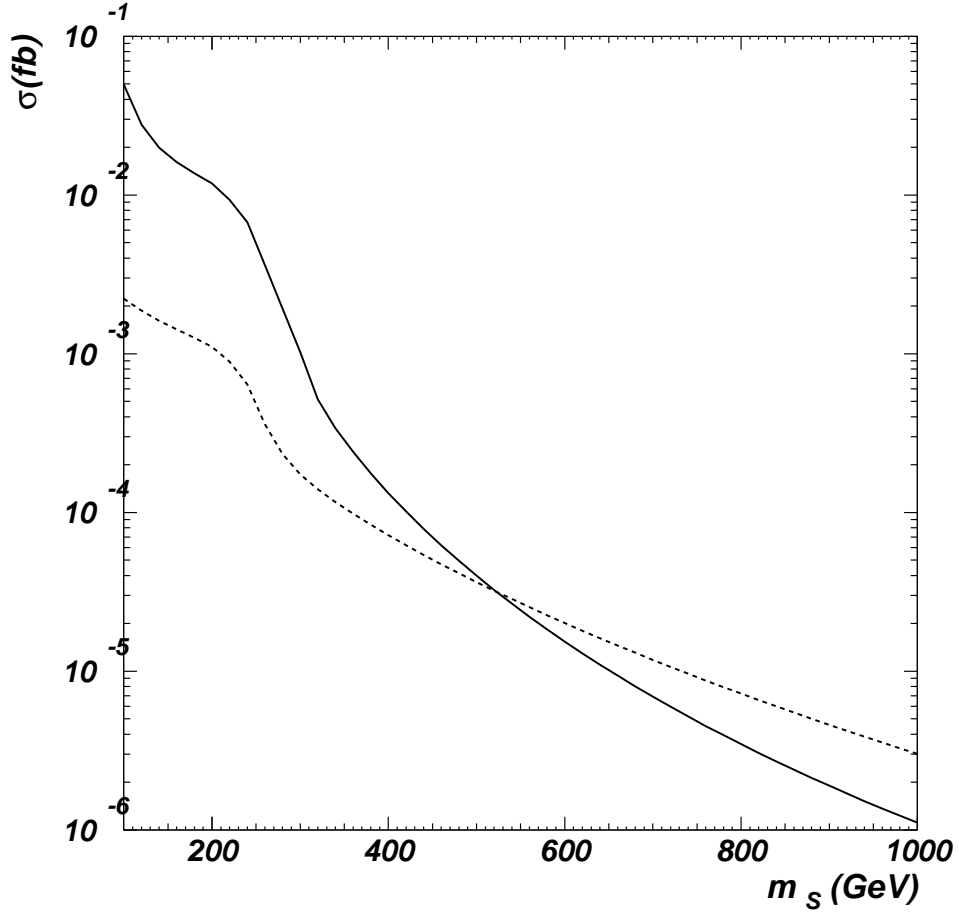


FIG. 2. The cross section for the process $e^+e^- \rightarrow t\bar{c}$ as a function of m_S , where $\sqrt{S} = 500\text{GeV}$, $\tan\beta = 2$, $\epsilon^2 = 1/4$ and $\mu = -100\text{GeV}$. The solid and dashed lines represent $m_{\tilde{g}} = 100\text{GeV}$ and 500GeV , respectively.

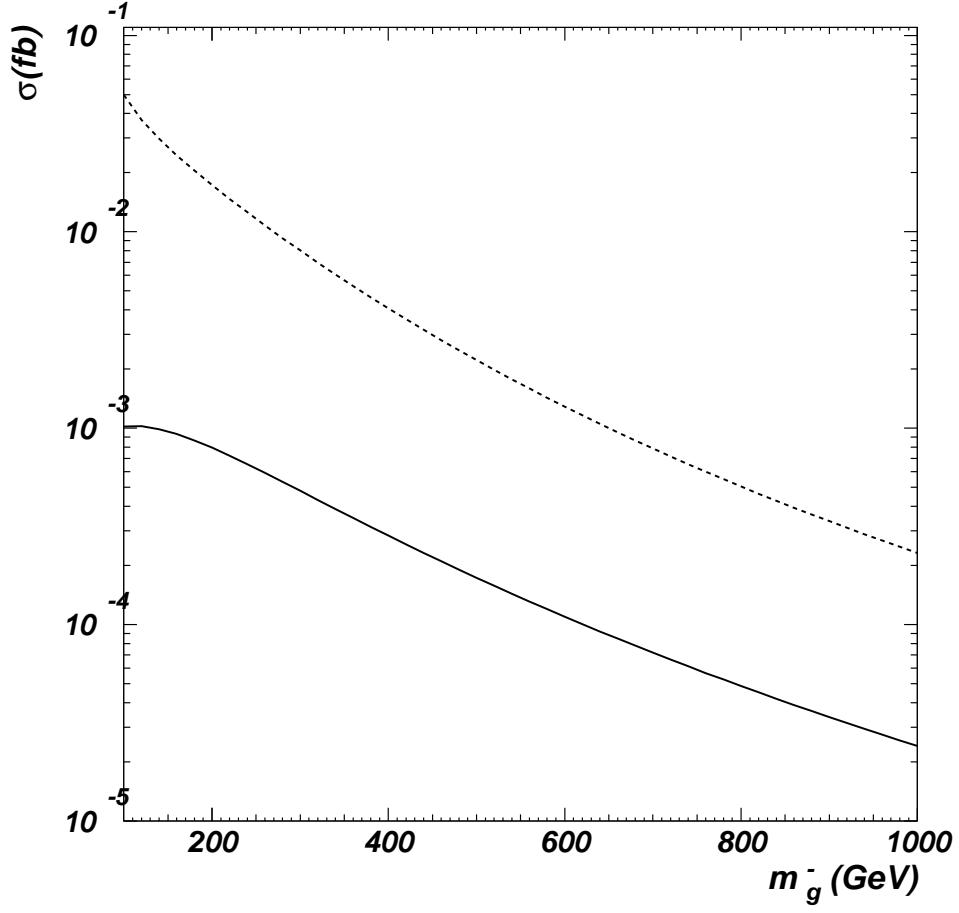


FIG. 3. The cross section for the process $e^+e^- \rightarrow t\bar{c}$ as a function of $m_{\tilde{g}}$, where $\sqrt{S} = 500\text{GeV}$, $\tan\beta = 2$, $\epsilon^2 = 1/4$ and $\mu = -100\text{GeV}$. The solid and dashed lines represent $m_S = 300\text{GeV}$ and 100GeV , respectively.

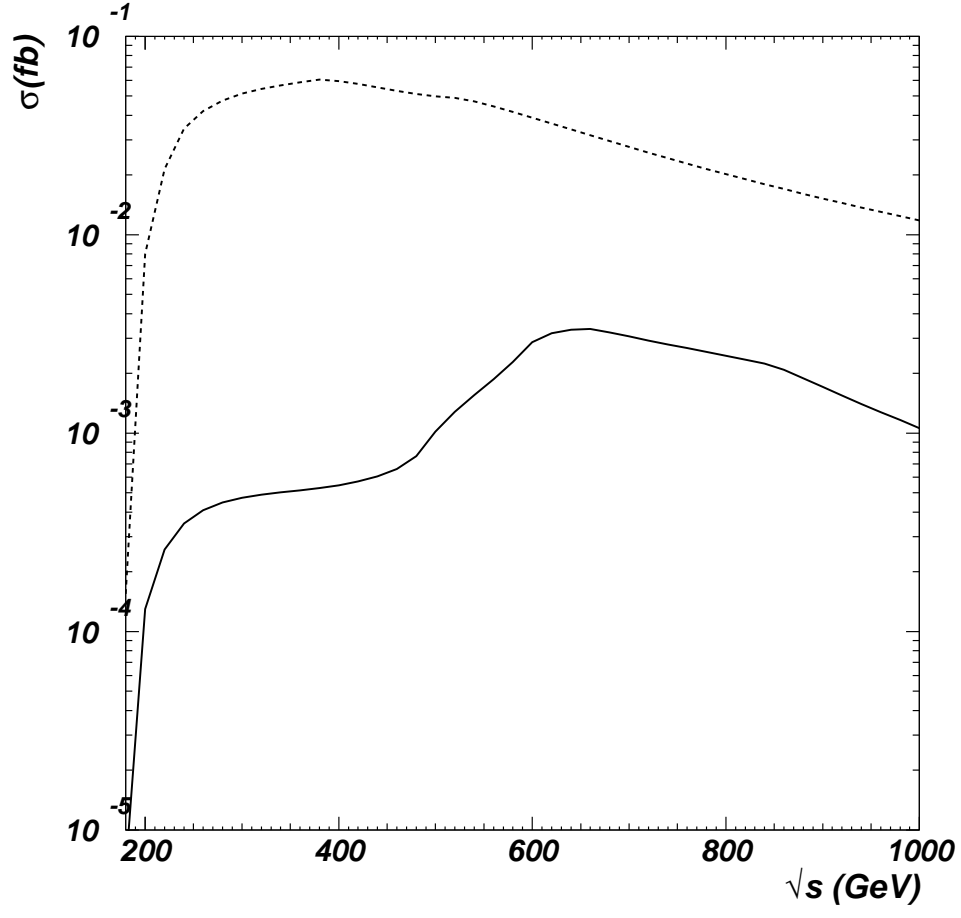


FIG. 4. The cross section for the process $e^+e^- \rightarrow t\bar{c}$ as a function of \sqrt{S} , where $m_{\tilde{g}} = 100\text{GeV}$, $\tan\beta = 2$, $\epsilon^2 = 1/4$ and $\mu = -100\text{GeV}$. The solid and dashed lines represent $m_S = 300\text{GeV}$ and 100GeV , respectively.

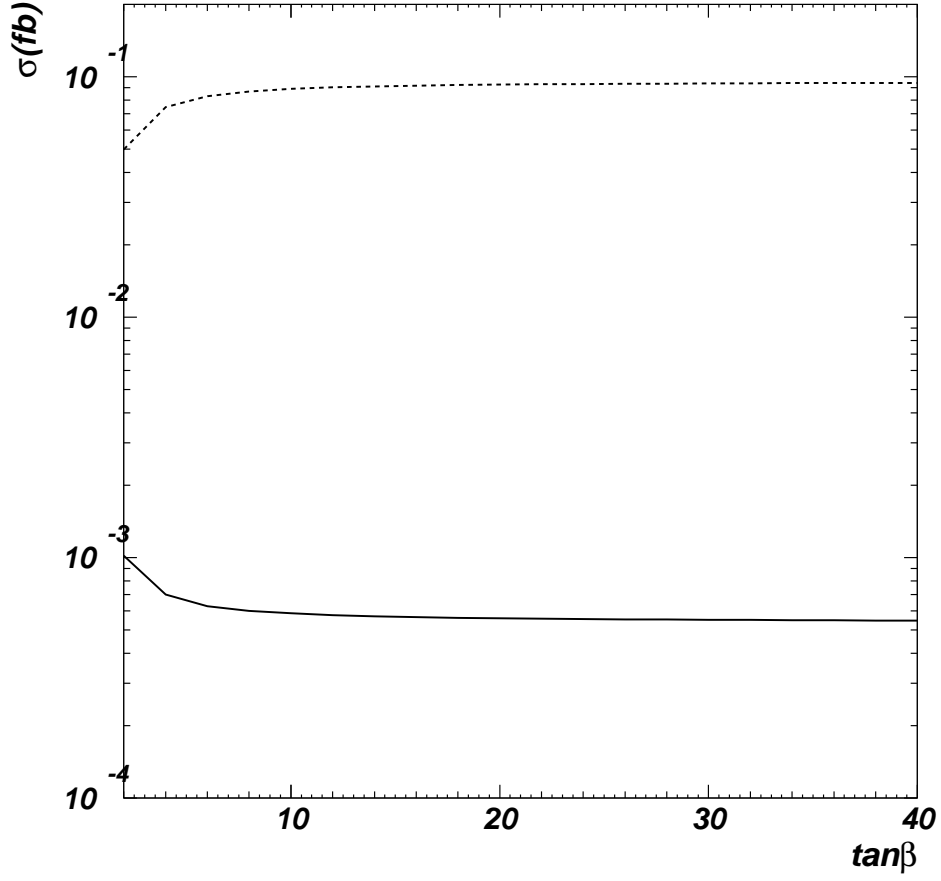


FIG. 5. The cross section for the process $e^+e^- \rightarrow t\bar{c}$ as a function of $\tan \beta$, where $\sqrt{S} = 500 GeV$, $m_{\tilde{g}} = 100 GeV$, $\epsilon^2 = 1/4$ and $\mu = -100 GeV$. The solid and dashed lines represent $m_S = 300 GeV$ and $100 GeV$, respectively.